Date of publication SEP-30, 2024, date of current version JUL-05, 2024.
www.computingonline.net / computing@computingonline.net

Print ISSN 1727-6209
Online ISSN 2312-5381
DOI 10.47839/ijc.23.3.3656

A Hybrid Method Based on Haris Corner and Maximally Stable Extremal Regions for Vehicle Plate Number Detection

BUDI SETIYONO, DWI RATNA SULISTYANINGRUM, DARMAJI, KOMAR BAIHAQI, WAHYU ARDIANSYAH

Department of Mathematics, Institut Teknologi Sepuluh Nopember, Surabaya, Indonesia

Corresponding author: Budi Setiyono (e-mail: masbudisetiyono@gmail.com).

This work was supported by Direktorat Riset dan Pengabdian Kepada Masyarakat (DRPM), Institut Teknologi Sepuluh Nopember dan Kementerian Pendidikan, Kebudayaan, Riset, dan Teknologi sesuai dengan Perjanjian Pelaksanaan Penelitian Keilmuan Dana ITS Batch 2 Tahun 2022 Nomor 1633/PKS/ITS/2022 tanggal 24 Mei 2022.

ABSTRACT An intelligent transportation system (ITS) is a crucial element of a smart city, and it includes the capability to identify vehicle license plates. Utilizing digital image processing is a cost-effective method for identification. The tiny size of the number plate is just one of the many unfortunate difficulties with this approach. Hence, this research is crucial, particularly in enhancing the precision of detection. The Harris Corner approach is one way to locate the motor vehicle number plate location. However, the Harris corner method could be more optimal for analyzing moving vehicle videos as input. Since frame-by-frame variations in the video input's lighting, accuracy cannot be maximized. Furthermore, the vehicle and license plate appear significantly smaller due to the camera's distant positioning. Consequently, the authors suggest a hybrid approach using the Maximally Stable Extremal Regions (MSER) method. The Harris Corner and MSER methods will concurrently identify the initial position of the vehicle number plate. Moreover, the initial detection outcomes of the two techniques are compared and adjusted to achieve a more precise determination of the placement of the number plate. The results show that integrating the MSER method into the Harris Corner method yields a hybrid approach that enhances accuracy by 13%. Furthermore, it visually represents the selected number plate with greater accuracy.

KEYWORDS Smart city; License plate detection; Harris Corner Method; Maximally Stable Extremal Regions method; matching and alignment.

I. INTRODUCTION

TODAY'S smart cities are overgrowing, and one of the components is the Intelligent Transportation System. [1–4]. Nowadays, digital image processing contributes significantly to various aspects of life, for example, in the health sector [5] and the transportation sector. Studies in the Intelligent Transportation System include detecting, identifying, and automating moving vehicles on the highway. Automation of vehicles is carried out by calculating the number of vehicles, detecting vehicle speed, and classifying vehicle types [6–9]. There are several ways to identify vehicles, including headlight detection [10–15], and a combination of vehicle shapes and sizes [16]. The most appropriate vehicle identification process is carried out by detecting the vehicle number plate because it is a visible and unique vehicle identity, making it possible to track the vehicle.

Detection of vehicle number plates can use monitoring cameras widely installed on the highway. Vehicle license plates from video data obtained from the camera can be detected using digital image processing. Researchers use various methods to detect license plates automatically, including the LVQ Neural Network [17, 18], Deep Neural Network [19], Convolution Network [20], Deep Learning [21–24], Yolo [25–27] and other methods [28]–[30]. One of the critical steps before doing number plate recognition is detecting the location of the license plate. This step must be accurate because it will affect the recognition process. Some researchers use the Haris Corner [31–34] and Maximally Stable Extremal Regions (MSER) [35–37] methods to detect the location of vehicle number. However, the two methods are carried out separately. In fact, according to the author, the Harris Corner and the MSER methods can complement the shortcomings of the two methods.

The author divides the presentation of this paper as follows: part 2 describes several existing methods related to the topic to be discussed, and part 3 presents the proposed method, as well as some fundamental theories used for this research.

Furthermore, section 4 is an experiment with its discussion; section 5 is a conclusion.

II. RELATED WORKS

Numerous research studies have used The Harris corner approach to detect vehicle number plates. More specifically, research on number plate detection performed by Tjendra Panchal, et al. aims to detect and segment vehicle license plates using the Harris Corner, considering that the brightness condition will not affect the image angle [38]. Based on this research, the conclusion is that the Harris Corner method can detect license plates in various brightness conditions. However, if there is a reflected effect of sunlight, it will complicate the detection process.

Because the Harris corner approach is compatible with rotationally altered images, other researchers utilize it to locate car number plates. In his research, the area of the number plate is detected by identifying the angular position of the text first [33]. In this study, the number plate used came from the vehicle's image with the stop position, and the focus of image capture was on the vehicle number plate.

Meanwhile, Yuan Feng studied to improve the Harris corner method based on the principle analysis of the Harris angle detection algorithm, the sub-pixel level angular position based on the Gauss surface extracted method. [31]. In this study, the detection of the angle of an object has been successfully improved. In this research, the detection of the curve of an object has been enhanced. Another researcher, Li-Yi Bo, designed a new Harris multi-scale angle detection algorithm based on contourlet transformation [34].

Another researcher, Michael Donoser et al., uses the Maximally Stable Region method to track objects. The component tree is an efficient data structure, enabling MSER calculations in quasi-linear time [37].

Meanwhile, other researchers used MSER for edge clustering and formulated it for the first time to solve plate detection. This research is also a new application of the most stable extreme region. [35]. In the research, Maulana et al. used MSER to detect the text on the vehicle's license plate, but the vehicle stopped, so the license plate looked very clear. [36].

From these studies, no researcher has combined the Harris Corner method and the MSER method to detect vehicle number plates. Moreover, the detection of the location of the number plate on the vehicle moving across the highway. Therefore, in this study, the authors propose a hybrid method, namely the Harris Corner method and the Maximally Stable Extremal Regions (MSER) method, which is carried out in parallel. The detection results of the two approaches will be matched and harmonized to increase accuracy in number plate detection. The MSER method is used because this method can segment characters under various conditions. The data used in this study is the result of video acquisition of vehicles moving on the highway.

III. PROPOSED METHODS

The block diagram in Figure 1 illustrates the steps of the research approach that the author proposes. The camera records a video of a vehicles in motion on a roadway and functions as the input for the system. Frames will be extracted from the video. Subsequently, the author establishes a Region of Interest (ROI) in Figure 2. The term "region of interest," or ROI, refers to the area of the image that the computer will process. ROI is necessary as it allows for the selective analysis of specific pixels in the image, reducing computing costs. Creating a rectangular shape in the video (image) frame area is the first step in determining the ROI.

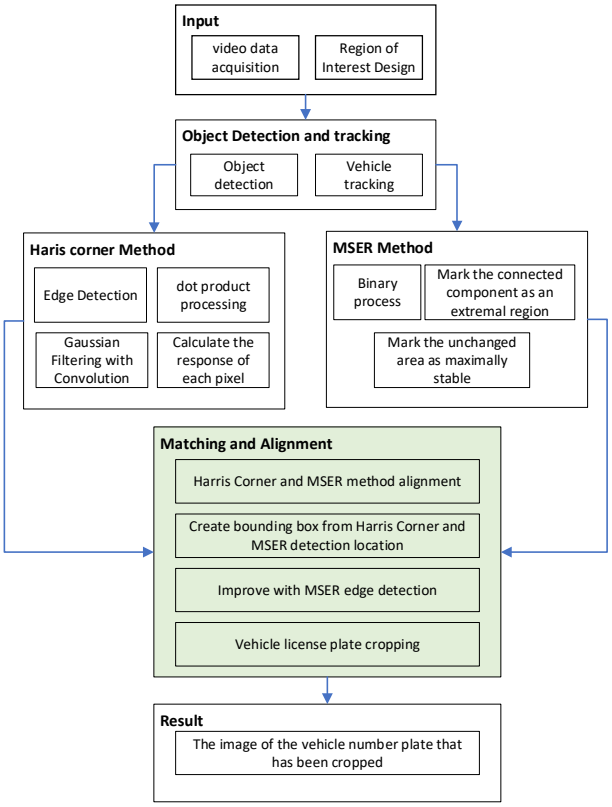

Figure 1. Research Methodology

A. OBJECT DETECTION AND TRACKING

The next stage is identifying objects by subtracting the background image from the foreground picture. A background image is taken while there are no cars on the road. To accelerate computational processes, the author converts the image into grayscale. Each frame decreases the background and foreground visuals. Differentiating between the foreground and background images is essential in enhancing the visibility of the vehicle item. They may be smaller when the background and foreground images have exact proportions. This technique is usually expressed by equation (1).

$$(i,j) = |A(i,j) - B(i,j)|, \quad (1)$$

where $P(i,j)$: Result Matrix; $A(i,j)$: Frame matrix, $B(i,j)$: Background matrix. This process is illustrated in Figure 2.

(a)

(b)

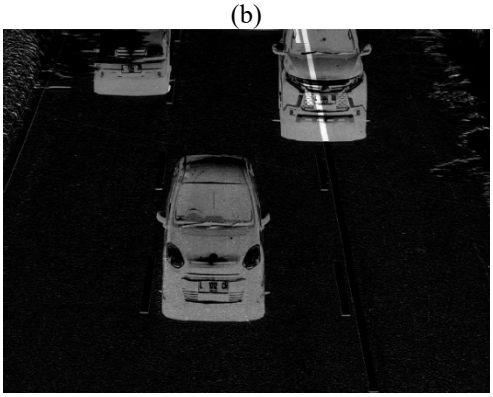

(c)

Figure 2. (a) image with foreground (b) image background (c) result of subtracting foreground with background

In Figure 2(c), we will use thresholding to make the item appear more distinct. A grayscale image is transformed into a binary image using thresholding. Thresholding has the mathematical definition given in equation (2) below:

$$g(x,y) = \begin{cases} 1, & \text{if } f(x,y) \geq T \\ 0 & \text{if } f(x,y) < T \end{cases}, \qquad (2)$$

where $g(x,y)$: thresholding image; and (x,y): grayscale image. Figure 4 displays the thresholding results; the object becomes more visible when the threshold value T=15 is used. The next step is image segmentation, which classifies images according to their intensity (differentiating between black and white), whether they are of vehicles in motion or other objects.

The next stage involves the implementation of vehicle tracking. At the moment, things detected are labelled to join them in a frame. Every item is assigned a distinct label beginning with the number 0. Each object label is distinct. Object tracking utilizes data about an object's spatial coordinates and reference frame. The author compares the object's position in the current frame and its position in the previous frame. An item is considered the same if its intersection between the current and previous frames can be detected. Therefore, it is given the identical label as the frame that came before it. If there is no collision, the objects will be assigned a new label in the specified order. Figure 4 illustrates the results of this method.

B. HARRIS CORNER METHOD

The Harris Corner method can accurately identify the position of the license plate on the recognized and labelled car object. Below are the algorithms for detecting a Harris corner:

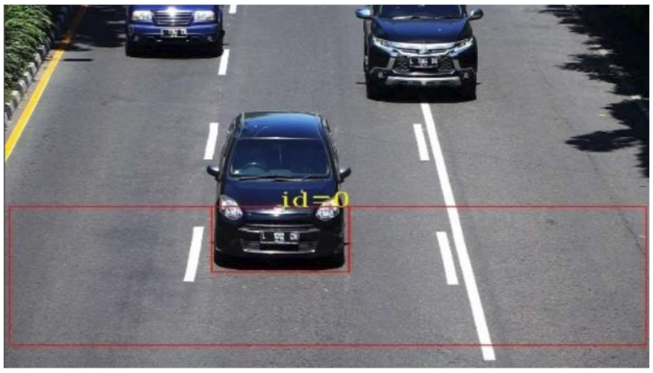

Figure 3. Tracking and labeling of detected objects

(i) Compute the image's derivatives. The goal of the derivative is to identify the image's vertical and horizontal edges. Convolution is the term for this method in image processing. The convolution is expressed mathematically in equation 3.

$$g(x,y) = \sum_{k=-w}^{w} \sum_{k=-w}^{w} h(k,l) f(m-k, n-l), \quad (3)$$

where $g(x,y)$ is the result of the convolution at coordinates (x,y), w is the size of the derivative kernel, and $h(k,l)$ is the derivative kernel at coordinates (k,l). Meanwhile, $(m-k,n-l)$ is the image that will be convoluted at the coordinates $(m-k,n-l)$. The Prewitt kernel from equation 4 will be applied in this procedure.

$$dx = \begin{bmatrix} -1 & 0 & 1 \\ -1 & 0 & 1 \\ -1 & 0 & 1 \end{bmatrix}; \; dy = \begin{bmatrix} -1 & -1 & -1 \\ 0 & 0 & 0 \\ 1 & 1 & 1 \end{bmatrix}. \qquad (4)$$

The convolution results using the Prewitt kernel are displayed in Figure 4.

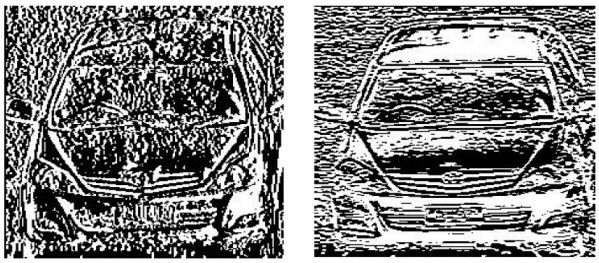

Figure 4. Convolution results with Prewitt kernel.

(ii) Determine the derivative dot product at every pixel. The dot product computation is expressed mathematically as follows in equation 5 :

$$h(x,y) = f(x,y).g(x,y), \qquad (5)$$

Suppose I_x the derivative of x and I_y is the derivative of y, then the formula for the dot product of the two is formulated as follows :

$$I_x^2 = I_x \cdot I_x \; ; \; I_y^2 = I_y \cdot I_y \; ; \; I_{xy} = I_x \cdot I_y; \qquad (6)$$

(iii) Gaussian filter convolution. Then, the Gaussian kernel will convolute once more, and get S_x^2, S_y^2, S_{xy}

(iv) Compute the response of each pixel using the Plessey operator. First, each pixel in the images S_x^2, S_y^2, and S_{xy} is taken and then defined into a matrix $H(x, y)$ with the following rules:

$$H = \begin{bmatrix} S_x^2(m,n) & S_{xy}(m,n) \\ S_{xy}(m,n) & S_y^2(m,n) \end{bmatrix}, \quad (7)$$

Equation 8 was then applied to determine each pixel's response.

$$R = \det(H) - k(tr(H))^2, \quad (8)$$

where R is a Plessey value; det (H) is the determinant of the matrix, and; is a constant (here we use = 0.01); $tr(H)$ is a trace matrix. For example, suppose S_x^2, S_y^2, and S_{xy} are as follows.

$$S_x^2 = \begin{bmatrix} 3 & 1 & 0 & 0 \\ 5 & 2 & 0 & 0 \\ 5 & 2 & 0 & 0 \end{bmatrix},$$

$$S_y^2 = \begin{bmatrix} 3 & 5 & 5 & 5 \\ 1 & 1 & 2 & 2 \\ 0 & 0 & 0 & 0 \end{bmatrix},$$

$$S_{xy} = \begin{bmatrix} 9 & 3 & 0 & 0 \\ 3 & 1 & 0 & 0 \\ 0 & 0 & 0 & 0 \end{bmatrix}. \quad (9)$$

In order to determine the pixel response (1,1), take the values, S_x^2 (1,1) = 3, S_y^2 = 3 and S_{xy} (1,1) = 9 we get :

$$H = \begin{bmatrix} 3 & 9 \\ 9 & 3 \end{bmatrix},$$
$$R = \det\left(\begin{bmatrix} 3 & 9 \\ 9 & 3 \end{bmatrix}\right) - k\left(tr\left(\begin{bmatrix} 3 & 9 \\ 9 & 3 \end{bmatrix}\right)\right)^2, \quad (10)$$
$$= -72 - 0.01 \times 36 = -72.36.$$

Similarly, the same process is applied to the remaining pixels. Therefore, the result is as follows:

$$R = \begin{bmatrix} -72.36 & -4.36 & -0.25 & -0.25 \\ -4.36 & 0.91 & -0.04 & -0.04 \\ -0.25 & -0.04 & 0 & 0 \end{bmatrix}. \quad (11)$$

(v) Determine the non-maximum suppression. Among all the detected edge pixels, this phase aims to determine the pixel whose position is nearest to the location where the pixel changed. For example, if R the Plessey value of a specific location is the highest value inside a rectangle $n \times n$, and n, which is determined through experimental means, is n=3 in this case. Therefore, this particular location can be referred to as a corner point.

$$R = \begin{bmatrix} \mathbf{-72.36} & \mathbf{-4.36} & \mathbf{-0.25} & \mathbf{-0.25} \\ \mathbf{-4.36} & \mathbf{0.91} & \mathbf{-0.04} & \mathbf{-0.04} \\ \mathbf{-0.25} & \mathbf{-0.04} & \mathbf{0} & \mathbf{0} \end{bmatrix}.$$

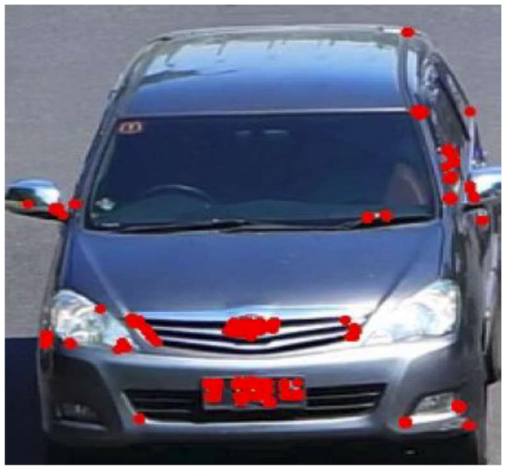

Figure 5. Harris Corner detection results

So, it is concluded that the coordinates (2,2) are corner points, and then the coordinates are stored. The results of Harris Corner are presented in Figure 5.

C. MSER METHOD

The authors used the MSER approach to concurrently identify text regions by searching for the most extensive and consistent area. This step is pragmatic since the text colour on the license plate is typically consistent. The MSER area is accepted if it satisfies specific criteria, which are as follows:

(i) Extensive area (MaxArea parameter),
(ii) Minimal area (MinArea parameter),
(iii) Volatile area (delta parameter).

The steps in the MSER method are as follows:

(i) Adjust the threshold by modifying the value from 0 to 255. Due to the generally uniform colour of the text on the license plate, this process step seeks to identify extreme locations. The results of this procedure are displayed in Figure 6.

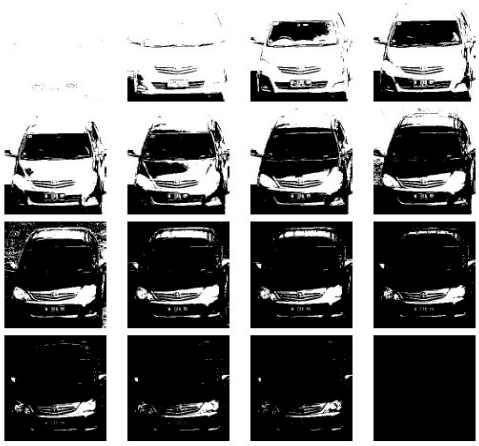

Figure 6. Thresholding Results

(ii) Identify and define the region associated with each threshold value. Any alteration in the threshold value will inevitably lead to a modification in the related component within the thresholding result. Consequently, there will be no need to threshold these areas. Figure 7 displays the result of this procedure.

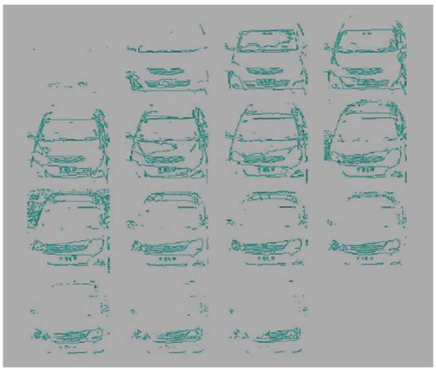

Figure 7. The result of determining the connected component

(iii) Calculate the maximum feasible area. The subsequent step determines the largest stable area, saving the extreme zones. This region is acquired by picking the largest throughout shifting thresholds. The parameters used are minArea = 10, maxArea = 90 and delta = 4. So the MSER area is obtained as shown in Figure 8.

Figure 8. MSER Area

Figure 8 shows that the plate area is marked as the MSER area, so it is used in detecting number plates.

D. MATCHING AND ALIGNMENT

Furthermore, the authors modify the detection results for the two approaches according to the empirical results.

Based on the vehicle images, the Harris Corner detection identifies the central region of the car plate as the most crucial location, as indicated by the yellow circle in Figure 9.

Figure 9. The widest area of the Harris Corner method detection results

The following phase verifies the area's location in Figure 9 to ensure it is also classified as an MSER area. Figure 10 depicts the checks.

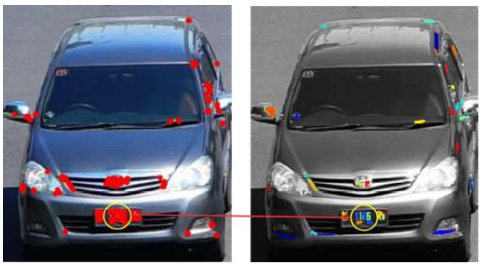

Figure 10. Matching process

If these criteria are satisfied, a bounding box will be created in the Harris Corner region. The box's width will be adjusted to match the length of the license plate, which is roughly 20 pixels to the right and left. To obtain the results as shown in Figure 11.

Figure 11. Number plate cropping results

The final step is to improve the outcomes derived from the preceding location, where the plate results rely solely on the identified Harris Corner region. To complete this stage, MSER is used to detect the plate edge. Figure 12 represents a number plate that the program has identified.

Figure 12. Detected plates

Figure 12 displays the results of the MSER obtained from the license plate. If the area is subtracted from the outside contour, it will yield the area enclosed by the white line of the plate. Subsequently, the method is depicted in Figure 13.

(a) (b)

Figure 13. Improvement results with plate line detection

IV. EXPERIMENT AND RESULT

A. DATA

Table 1 displays the necessary information used in the research. Primary data was collected by acquiring experimental data by video data capture using a camera positioned directly on the highway.

Table 1. Experimental Data

No.	Experimental data	Location
1	Video 1	Jembatan penyeberangan Cito, Jl. Ahmad Yani – 1
2	Video 2	Jembatan penyeberangan depan UINSA, Jl. Wonokromo
3	Video 3	Jembatan penyeberangan taman Pelangi, Jl. Ahmad Yani
4	Video 4	Jembatan penyeberangan Cito, Jl. Ahmad Yani – 2

Figure 14 illustrates the placement of a camera to obtain information. The camera is placed on the road and is pointed at the car; meanwhile, the vehicle approaches the observer.

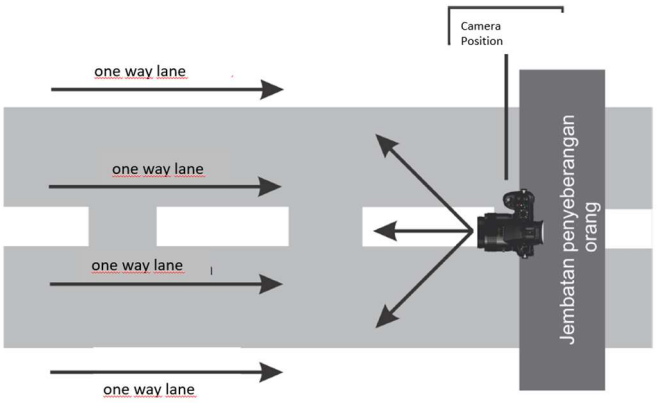

Figure 14. Camera positioning during the collection of data

A video of moving vehicles has been taken in clear weather. The video resolution is 1440 x 1080 pixels with a frame rate of 25 frames/second for 2 minutes. The following is a list of experiment inputs

B. RESULT

In these studies, license plate detection relies on the presence of a recognized car object. The number of plates that must be detected is equal to the number of vehicles captured. Table 2 presents the data regarding the experiments conducted on the four videos.

Table 2. Accuracy of test results

Experimental data	Methods	Category	JS	JT	TT	SD
Video 1	Hybrid	Vehicle	89	83	6	1
		Plate	83	69	2	12
	Non Hybrid	Vehicle	89	83	6	1
		Plate	83	69	2	12
Video 2	Hybrid	Vehicle	40	40	0	0
		Plate	40	34	0	6
	Non Hybrid	Vehicle	40	40	0	0
		Plate	40	34	0	6
Video 3	Hybrid	Vehicle	54	44	10	5
		Plate	44	35	2	7
	Non Hybrid	Vehicle	54	44	10	5
		Plate	44	35	2	7
Video 4	Hybrid	Vehicle	74	68	6	0
		Plate	68	55	5	8
	Non Hybrid	Vehicle	74	68	6	0
		Plate	68	55	5	8

Where JS – Actual Number; JT – Number of Detected; TT – Not Detected; SD – Wrong Detection.

The validation process is carried out empirically by comparing the results of detection by the system with actual conditions. Two items to be observed, namely recall and precision

$$recall = \frac{number\ of\ plates\ detected}{Actual\ number\ of\ vehicles} x100\% , \quad (12)$$

$$precision = \frac{number\ of\ plates\ detected}{number\ of\ vehicles\ detected} x100\% . \quad (13)$$

Table 3 presents the computation of recall and precision for the experimented-on data. Figure 10 shows the graphical representation of recall and precision results.

Table 3. Test results for 4 videos

Experimental data	Methods	Recall	Precision
Video 1	Hybrid	77.53%	83.13%
	Non Hybrid	77.53%	83.13%
Video 2	Hybrid	85%	85%
	Non Hybrid	85%	85%
Video 3	Hybrid	64.81%	79.54%
	Non Hybrid	64.81%	79.54%
Video 4	Hybrid	74.32%	80.88%
	Non Hybrid	74.32%	80.88%

Compared to the other three videos, video 3 yields the lowest recall and precision numbers, as seen from the findings above. Due to the proximity of multiple vehicles in video 3, the algorithm categorizes them as a single entity. Furthermore, the camera moves due to wind and vibrations on the pedestrian bridge; as a result, a portion of the background in specific frames is seen as an object. The chart also indicates that hybrid or non-hybrid plates have no impact. The table illustrates the disparities in the number of plates effectively restored using MSER.

Table 4 presents the outcomes of the cropping tests, visually displaying the results with and without using hybrids. The ID illustrates the frame number the system selected as having optimal outcomes.

Table 4. Visual representation of number plate crop

Id	Experimental data	Non Hybrid	Hybrid
9	Video 1		
68	Video 1		
27	Video 2		
34	Video 2		
34	Video 3	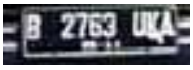	
36	Video 3		

43	Video 4		
61	Video 4		

By comparing the non-hybrid and hybrid methods to the plate number ratio, the error rate of plate detection can be determined, depending on the actual plate size. The ratio formula is expressed by equation 5.3. The standard length of a motor vehicle license plate in Indonesia, as determined by ground truth, is 45 cm, while the height of the plate is 13 cm. The standard plate ratio is 3.46. This ratio will be used to compare it with the ratio generated by the system. The author determines the ratio precision using the following formula 14:

$$ratioGt = \frac{length\ of plate}{width\ of\ plate}. \quad (14)$$

Table 5 displays the computation for obtaining the Mean Square Error. The accuracy computation involves comparing the vehicle number plate ratio generated by the system with the actual vehicle number plate ratio, known as the ground-truth ratio (ratioGt), multiplied by 100%.

$$MSE = \sum \frac{(ratio - ratioGt)^2}{n}. \quad (15)$$

Table 5. MSE accuracy for the number plate ratio.

Experimental data	Method $(ratio - ratioGt)^2$	
	Non Hybrid	Hybrid
video 1 (9)	0,4356	0,0036
video 1 (68)	0,0256	0,0001
video 2 (27)	0,0016	0,0001
video 2 (34)	0,3969	0,2916
video 3	0,1089	0,0225
video 3	0,0625	0,5776
video 4	0,4624	0,1849
video 4	0,9409	0,2916
Sum	**2,4344**	**1,3720**
MSE	**0,3043**	**0,1715**

The mean square error has been reduced from 0.3043 to 0.1715, resulting in a decrease in error of 0.1328. Figure 15 shows our method's successful reduction of error in the number plate area.

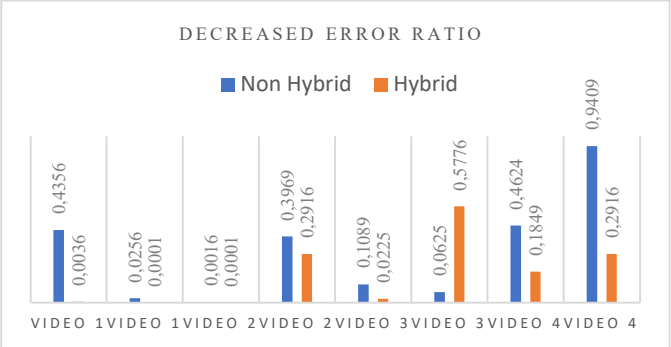

Figure 15. Diagram showing the accuracy increase after applying MSER

V. CONCLUSION

Based on our experiment, the authors conclude that the suggested hybrid method can improve the accuracy of the number plate position detection findings. This phenomenon can be observed by employing a hybrid approach, which results in a significant decrease of 13% in the error rate. Nevertheless, hybrid and non-hybrid approaches had little impact on the number of plates detected. Consequently, the number plate is visible when a car object is detected, but with imprecise results.

References

[1] V. Albino, U. Berardi, and R. M. Dangelico, "Smart cities: definition, deminsion, and performance," *J. Urban Technol.*, vol. 22, pp. 3–21, 2015, https://doi.org/10.1080/10630732.2014.942092.

[2] S. Fiore *et al.*, "An integrated big and fast data analytics platform for smart urban transportation management," *IEEE Access*, vol. 7, pp. 117652–117677, 2019, https://doi.org/10.1109/ACCESS.2019.2936941.

[3] I. Gulati and R. Srinivasan, "Image processing in intelligent traffic management," *Int. J. Recent Technol. Eng.*, vol. 8, no. 2, special issue 4, pp. 213–218, 2019, https://doi.org/10.35940/ijrte.B1040.0782S419.

[4] K. Iqbal, M. A. Khan, S. Abbas, Z. Hasan, and A. Fatima, "Intelligent transportation system (ITS) for smart-cities using Mamdani fuzzy inference system," *Int. J. Adv. Comput. Sci. Appl.*, vol. 9, no. 2, pp. 94–105, 2018, https://doi.org/10.14569/IJACSA.2018.090215.

[5] A. Çevik, G. W. Weber, B. M. Eyüboğlu, and K. K. Oğuz, "Voxel-MARS: a method for early detection of Alzheimer's disease by classification of structural brain MRI," *Ann. Oper. Res.*, vol. 258, no. 1, pp. 31–57, 2017, https://doi.org/10.1007/s10479-017-2405-7.

[6] A. Crouzil, L. Khoudour, P. Valiere, and D. N. Truong Cong, "Automatic vehicle counting system for traffic monitoring," *J. Electron. Imaging*, vol. 25, no. 5, p. 051207, 2016, https://doi.org/10.1117/1.JEI.25.5.051207.

[7] B. Setiyono, D. R. Sulistyaningrum, Soetrisno, and D. W. Wicaksono, "Multi vehicle speed detection using euclidean distance based on video processing," *Int. J. Comput.*, vol. 18, no. 4, pp. 431–442, 2019, https://doi.org/10.47839/ijc.18.4.1613.

[8] B. Setiyono, R. D. Susanti, D. R. Sulistyaningrum, and I. G. N. Usadha, "Classification and counting of moving vehicle at night with similarity of rear lamp," *J. Phys. Conf. Ser.*, vol. 1490, no. 1, pp. 1–13, 2020, https://doi.org/10.1088/1742-6596/1490/1/012044.

[9] F. M. D. S. Matos and R. M. C. R. De Souza, "An image vehicle classification method based on edge and PCA applied to blocks," *Conf. Proc. – IEEE Int. Conf. Syst. Man Cybern.*, pp. 1688–1693, 2012, https://doi.org/10.1109/ICSMC.2012.6377980.

[10] S. Kanagamalliga, S. Vasuki, A. Kanimozhidevi, S. Priyadharshni, and S. Rajeswari, "Tracking and counting the vehicles in night scenes," *Int. J. Inf. Sci. Tech.*, vol. 4, no. 3, pp. 165–172, 2014, https://doi.org/10.5121/ijist.2014.4320.

[11] S. Padmavathi, C. R. Naveen, and V. Ahalya Kumari, "Vision based vehicle counting for traffic congestion analysis during night time," *Indian J. Sci. Technol.*, vol. 9, no. 20, pp. 1–6, 2016, https://doi.org/10.17485/ijst/2016/v9i20/91742.

[12] C. Tang, Y. Dong, X. Lin, and W. Xiao, "Multi-field depth vehicle headlight detection by model construction and long trajectory extraction in nighttime city traffic," *Smart Innov. Syst. Technol.*, vol. 62, pp. 234–246, 2017, https://doi.org/10.1007/978-981-10-3575-3_24.

[13] B. G. Rajagopal, "Detection and pairing of vehicle headlight in night scenes," *Int. J. Res. Eng. IT Soc. Sci.*, vol. 3, no. 9, pp. 37–53, 2018.

[14] W. Zhang, Q. M. J. Wu, G. Wang, and X. You, "Tracking and pairing vehicle headlight in night scenes," *IEEE Trans. Intell. Transp. Syst.*, vol. 13, no. 1, pp. 140–153, 2012, https://doi.org/10.1109/TITS.2011.2165338.

[15] R. K. Sathish Kumar, N. Priya, "Vehicle speed computation in night scenes using headlight tracking and pairing," I*nternational Journal of Research in Engineering & Advanced Technology (IJREAT)*, vol. 2, no. 2, pp. 2–6, 2014.

[16] J. Trivedi, M. S. Devi, and D. Dhara, "Vehicle counting module design in small scale for traffic management in smart city," *Proceedings of the 2018 3rd Int. Conf. Converg. Technol. I2CT 2018*, April 2018, pp. 1–6, https://doi.org/10.1109/I2CT.2018.8529506.

[17] M. Z. Zheng and Q. Y. Liu, "Application of LVQ neural network to car license plate recognition," *Proceedings of the 2010 IEEE Int. Conf. Intell. Syst. Knowl. Eng. ISKE 2010*, pp. 287–290, 2010, https://doi.org/10.1109/ISKE.2010.5680862.

[18] A. P. Nagare, "License plate character recognition system using neural

network," *Int J Comput Appl*, vol. 25, no. 10, pp. 36–39, 2011. https://doi.org/10.5120/3147-4345/

[19] H. Li, P. Wang, M. You, and C. Shen, "Reading car license plates using deep neural networks," *Image Vis. Comput.*, vol. 72, pp. 14–23, 2018, https://doi.org/10.1016/j.imavis.2018.02.002.

[20] O. Ibitoye, T. Ejidokun, O. Dada, and O. Omitola, "Convolutional neural network-based license plate recognition techniques: A short overview," *Proceedings of the 2020 Int. Conf. Comput. Sci. Comput. Intell. CSCI 2020*, pp. 1529–1532, 2020, https://doi.org/10.1109/CSCI51800.2020.00283.

[21] T. Vetriselvi *et al.*, "Deep learning based license plate number recognition for smart cities," *Comput. Mater. Contin.*, vol. 70, no. 1, pp. 2049–2064, 2021, https://doi.org/10.32604/cmc.2022.020110.

[22] V. Gnanaprakash, N. Kanthimathi, and N. Saranya, "Automatic number plate recognition using deep learning," *IOP Conf. Ser. Mater. Sci. Eng.*, vol. 1084, no. 1, p. 012027, 2021, https://doi.org/10.1088/1757-899X/1084/1/012027.

[23] M. Shahidi Zandi and R. Rajabi, "Deep learning based framework for Iranian license plate detection and recognition," *Multimed. Tools Appl.*, vol. 81, no. 11, pp. 15841–15858, 2022, https://doi.org/10.1007/s11042-022-12023-x.

[24] W. Puarungroj and N. Boonsirisumpun, "Thai license plate recognition based on deep learning," *Procedia Comput. Sci.*, vol. 135, pp. 214–221, 2018, https://doi.org/10.1016/j.procs.2018.08.168.

[25] B. Setiyono, D. A. Amini, and D. R. Sulistyaningrum, "Number plate recognition on vehicle using YOLO – Darknet," *J. Phys. Conf. Ser.*, vol. 1821, no. 1, pp. 1–12, 2021, https://doi.org/10.1088/1742-6596/1821/1/012049.

[26] S. Obulakshmi, M. Ramya, and J. Mythili, "License plate detection using YOLO v4," *Int. J. Health Sci. (Qassim).*, vol. 6, no. March, pp. 5098–5111, 2022, https://doi.org/10.53730/ijhs.v6nS5.9741.

[27] R. Laroca *et al.*, "A robust real-time automatic license plate recognition based on the YOLO detector," *Proc. Int. Jt. Conf. Neural Networks*, vol. 2018, pp. 1–10, 2018, https://doi.org/10.1109/IJCNN.2018.8489629.

[28] S. Ozbay and E. Ercelebi, "Automatic vehicle identification by plate recognition," *World Acad. Sci. Eng. Technol.*, vol. 9, pp. 222–225, 2005.

[29] K. Horak, J. Klecka, and P. Novacek, "License plate detection using point of interest detectors and descriptors," *Proceedings of the 2016 39th Int. Conf. Telecommun. Signal Process. TSP 2016*, June 2016, pp. 484–488, https://doi.org/10.1109/TSP.2016.7760926.

[30] E. E. Etomi and D. U. Onyishi, "Automated number plate recognition system," *Trop. J. Sci. Technol.*, vol. 2, no. 1, pp. 38–48, 2021, https://doi.org/10.47524/tjst.21.6.

[31] Y. Han, P. Chen, and T. Meng, "Harris corner detection algorithm at sub-pixel level and its application," *Proceedings of the 2015 Int. Conf. Comput. Sci. Eng.*, vol. 17, no. ICCSE, pp. 133–137, 2015, https://doi.org/10.2991/iccse-15.2015.23.

[32] C. Luo, X. Sun, X. Sun, and J. Song, "Improved Harris corner detection algorithm based on Canny edge detection and Gray difference preprocessing," *J. Phys. Conf. Ser.*, vol. 1971, no. 1, 2021, https://doi.org/10.1088/1742-6596/1971/1/012088.

[33] F. A. Akbar and H. Maulana, "Detection of Indonesian vehicle plate location using Harris corner feature detector method," in *International Conference on Science and Technology*, 2018, vol. 1, no. Icst, pp. 877–881. https://doi.org/10.2991/icst-18.2018.177

[34] Y. B. Li and J. J. Li, "Harris corner detection algorithm based on improved contourlet transform," *Procedia Eng.*, vol. 15, pp. 2239–2243, 2011, https://doi.org/10.1016/j.proeng.2011.08.419.

[35] G. S. Hsu, J. C. Chen, and Y. Z. Chung, "Application-oriented license plate recognition," *IEEE Trans. Veh. Technol.*, vol. 62, no. 2, pp. 552–561, 2013, https://doi.org/10.1109/TVT.2012.2226218.

[36] H. Maulana, D. Herumurti, and A. Yuniarti, "Text based maximally stable extremal regions to detect vehicle plate location," *Proceeding of the International Joint Conference on Science and Technology (IJCST)*, 2017, pp. 450–455.

[37] M. Donoser and H. Bischof, "Efficient Maximally Stable Extremal Region (MSER) tracking," *Proceedings of the IEEE Comput. Soc. Conf. Comput. Vis. Pattern Recognit.*, 2006, vol. 1, pp. 553–560, https://doi.org/10.1109/CVPR.2006.107.

[38] T. Panchal, H. Patel, and A. Panchal, "License plate detection using Harris corner and character segmentation by integrated approach from an image," *Procedia Comput. Sci.*, vol. 79, pp. 419–425, 2016, https://doi.org/10.1016/j.procs.2016.03.054.

***Budi Setiyono** is a Assoc.Profesor in the Mathematics Department of the Institut Teknologi Sepuluh Nopember Indonesia. He received his B.Sc. in 1997 at the Mathematics Department, Institut Teknologi Sepuluh Nopember, M.Sc. in 2002 from Informatics Engineering, Institut Teknologi Bandung, and Ph.D. in 2012 from the Institut Teknologi Sepuluh Nopember. He is currently an Associate Professor at the Institut Teknologi Sepuluh Nopember., His research interests are digital image processing and computational mathematics*

***Dwi Ratna Sulistyaningrum** received a B.Sc. degree in mathematics and an M.Sc. in Informatics, both from the Institut Teknologi Bandung (ID), and a Ph.D. degree in 2013 from the Institut Teknologi Sepuluh Nopember (ID). She is currently a lecturer in the department of Mathematics and an Associate Professor at the Institut Teknologi Sepuluh Nopember (ID). Her research interests are in Image and video processing*

***Komar Baihaqi** received a B.Sc. degree in mathematics from the Institut Teknologi Sepuluh Nopember (ID) and a Master's degree from the Department of Mathematics, University of Gajah Mada, Indonesia. He is currently a lecturer in the department of Mathematics and an Assistant Professor at the Institut Teknologi Sepuluh Nopember (ID). Her research interests are in Matrix Computation and Algebra*

***Darmaji** received a B.Sc. degree in mathematics from Institut Teknologi Sepuluh Nopember (ID) M.Sc and a Ph.D. in Mathematics Department, both from the Institut Teknologi Bandung (ID). He is currently a lecturer in the department of Mathematics and an Assistant Professor at the Institut Teknologi Sepuluh Nopember (ID). His research interests are Graph Theory and Application.*

***Wahyu Ardiansyah** received a B.Sc. degree in mathematics from Institut Teknologi Sepuluh Nopember (ID). Currently, he works as an android developer at a software development company in East Java, Indonesia.*